This is to certify that the

thesis entitled

SEISMIC RESPONSE OF
TIED ARCH BRIDGES

presented by

Aida Bellamine

has been accepted towards fulfillment
of the requirements for

MS degree in Civil Engineering

R. K. Wen

Major professor

Date July 27, 1992

SEISMIC RESPONSE OF TIED ARCH BRIDGES

By

Aida Bellamine

A THESIS

Submitted to
Michigan State University
in partial fulfillment of the requirements
for the degree of

MASTER OF SCIENCE

Department of Civil and Environmental Engineering

1992

ABSTRACT

SEISMIC RESPONSE OF TIED ARCH BRIDGES

By

Aida Bellamine

The bridges were classified into heavy rib-light deck, light rib-heavy deck and medium rib-medium deck types. Their seismic responses based on the AASHTO design spectrum were found to be very close to the response average to three time history ground motions. The seismic effect relative to live load effect was expressed in terms of a "structural zone factor". An "optimal" distribution of the structural material between the arch and the deck was considered. An "optimal" value of the cross-sectional area ratio of deck to rib was found to range between 0.75 and 0.97. It was observed that except for the tensile stress from the deck tie rod action, the seismic responses of the tied and deck types of arch bridges were quite similar.

To my parents and brothers and sisters

for their love and support.

ACKNOWLEDGMENTS

I would like to thank Dr. Robert K. L. Wen, Professor of Civil Engineering at Michigan State University. Without his support and assistance, this work would not have been accomplished.

I would also like to thank the National Science Foundation for sponsoring the project. I would like to thank my committee members at Michigan State University: Dr. R. Harichandran, Dr. F. Hatfield and Dr. J. Lubkin.

TABLE OF CONTENTS

TABLE OF CONTENTS (Continued)

TABLE OF CONTENTS (Continued)

TABLE OF CONTENTS (Continued)

LIST OF TABLES

LIST OF FIGURES

LIST OF SYMBOLS

A = "bedrock" acceleration

AA = dead load compressive force divided by a "reference allowable stress", (see Equation 2.2)

ABAR = ratio of the deck cross-sectional area to the rib cross-sectional area

A_d = cross-sectional area of the deck

ALPHA = dead load factor divided by the rib slenderness ratio, (see Equation 2.4)

A_r = cross-sectional area of the rib

A_s = cross-sectional area of the suspenders

ASTAR = cross-sectional area of deck plus rib divided by "reference area AA", (see Equation 2.1)

BSMAXX = seismic amplification factor for straigth beam stress

C_d = deck half depth

C_r = rib half depth

D_d = deck depth

D_r = rib depth

E = Young' smodulus

f = stress

F_a = reference allowable stress

LIST OF SYMBOLS (continued)

g = acceleration of gravity

GAMMA = dead load factor in terms of the rib stiffness, (see Equation 2.14)

GSTAR = dead load factor in terms of the total stiffness (that of the deck plus that of the rib), (see Equation 2.3)

H = rise of arch

I_d = moment of inertia of deck

I_r = moment of inertia of rib

K = stiffness

L = span length

M = bending Moment

M = total mass per unit length

M_r = rib mass per unit length

N = number of panels

P = axial force

R_d = radius of gyration of deck section

R_r = radius of gyration of rib section

RHO = Ratio of deck bending stiffness to rib bending stiffness = I_d/I_r

S = section modulus

S = site (soil) coefficient

SA = spectral acceleration

SAM = ratio of axial stress to total stress

SMAXX = seismic amplification factor for curved beam stress

T_i = ith natural period

z_s = site zone factor

Z_{st} = "structural zone factor"

ξ = critical damping coefficient

1. INTRODUCTION

1.1 Motivation

Major earthquakes in recent years have caused significant damage to some highway bridges. Such damage could pose a threat to the life line system of which bridges are links. This consideration motivated a number of researchers to conduct studies on the behavior and response of highway bridges under seismic excitations. As far as arch bridges are concerned, much of the past work was done on the "deck type arched bridges" (Figure 5.1), (which, in order to avoid confusion with the general term of the deck of a bridge, will sometimes be referred to in the present study as the "D-bridges"). In terms of existing arch bridges, the tied type bridges (Figure 2.1), (which may be in this work referred to as the "T-bridges") are as frequently constructed as, if not more than, the D-bridges. A deck type arch bridge is usually built on rock foundations (e.g. crossing a gorge), while a tied arch bridge is built on softer soils (e.g. crossing a river). The purpose of this thesis is to investigate the seismic response of the tied type arch bridges.

Research on the deck type arch bridges was reported by Dusseau and Wen [1] who studied the in-plane and out-of-plane dynamic response of three actual deck type arch bridges under unequal as well as equal support motions. Inelastic responses of D-bridges were reported by Wen and Lee

[2]. R. J. Millies recently conducted a study on the effects of the lateral stiffness of the end towers on the seismic response of the D-bridges in the three dimensional space [3].

Work on tied arch bridges has been scarce. In 1989, Lee and Torkamani [4] conducted a study of the seismic resistance of tied arch bridges in the three dimensional space. It compared two mathematical models for the bridge deck. In the first one the bridge deck was modelled by a series of simple beam elements connected to the tension ties at panel points, in the second one the bridge deck system is represented by three dimensional super-elements, each treated as an independent substructure. The latter model can reflect the local bending of the individual deck stringers, while the former cannot. Phase-different wave ground motions and the flexibility of the soil surrounding the foundation were considered. It was found that the beam model of the deck system was not adequate to produce the seismic response in three dimensional space.The study was, however, conducted on a single existing bridge, which limits its generality.

1.2 Object and Scope

The objective of this thesis is to study the general characteristics of the seismic responses of the tied arch bridges. Attempts were also made in the study to assess the significance of such responses in design practice, and to relate them to those of the deck type bridges for which much more data are available.

The work for this study was based on computer modelling. The model used is a two dimensional one, dealing with the in-plane elastic behavior of bridges under equal support ground motions consisting of horizontal and vertical components. No soil-structure interaction was

accounted for. The system is assumed to be elastic. After having established that geometric nonlinearity has little effect on the seismic behavior of T-bridges, the problems were solved as linear ones. Eight panels were used in the bridge model, with uniform mass distribution on the horizontal projection. The cross-sectional area and the bending stiffness were assumed to be constant for each structural member set: rib, deck and suspenders. Young' s modulus was taken to be 29000 ksi. Three ground motion inputs were used for time history analysis, and the AASHTO [5] design spectrum was employed for spectral response analysis.

In the following, Chapter two describes the bridge model used and the parameters of the problem. An examination of the range of values of these parameters for some existing bridges resulted in a classification of tied arch bridges into three types; heavy rib-light deck, light rib-heavy deck and medium rib-medium deck. Based on this classification, three bridges were generated from each of three prototype bridges for the study. Chapter three reports an investigation of the seismic responses to three ground motion inputs and to the AASHTO [5] design spectrum. It was found that the average of the time history responses to the three ground motion inputs (the 1940 El Centro and the CIT B1 and B2 accelerograms [6]) was very close to the spectral analysis response based on the AASHTO [5] design spectrum. This reinforces the validity of that spectrum for design purposes. Also, in chapter three, a "structural zone factor" Z_{st} that compares the earthquake effects with the live load effects is developed.

In Chapter four, an exploratory study on an "optimal" distribution of structural material between the deck and the rib was conducted. It was based on the assumption that the "optimal" ratio of the cross-sectional areas of the deck to the rib is that for which the maximum stresses in the

rib and deck are equal. The value of that ratio was found to range from 0.75 to 0.97. Chapter five presents a comparative study of the T-bridges and the D-bridges, insofar as their dead load plus seismic responses are concerned. It was found that the responses of the two bridge types were quite close. Finally chapter six recapitulates the work done and presents the concluding remarks on this investigation.

2. MODELING AND PARAMETERS

2.1 General

This chapter describes the modeling and the parameters of the present study. In the first section, the bridge model used is described. In the second section, the static and dynamic loading are described. In the third section, the parameters of the study are enumerated. Finally, in the last section, seven existing bridges were considered. They were classified into three categories according to their design characteristics.

2.2 Modeling

The bridge model used in the present study (Figure 2.1) is a two dimensional elastic finite element model. The bridge is divided into eight panels of equal length. It has a roller support at the left end and a hinged support at the right end. The arch rib and deck are rigidly connected at the supports providing rotational as well as translational continuity. All loads and masses are lumped at the panel points.

2.2.1 Arch Rib

The rib is a parabolic arch represented by a series of curved beam elements [7] connected at the panel points. It is worth mentioning here that the larger the number of panels and hence the number of nodal points, the closer the (lumped) static load distribution approaches a uniform one. That would decrease the bending stresses. It is well known that bending stresses

vanish in a parabolic arch when the load distribution is uniform on its horizontal projection. The cross-sectional area and the moment of inertia are assumed to be the same for all arch rib curved beam elements, and constant along their lengths.

2.2.2 Deck

The deck is represented by a series of straight beam elements connected at panel points. It also acts as a tie which eliminates the need for thrust abutments. The cross-sectional area and the moment of inertia are assumed to be the same for all deck straight beam elements, and constant along their lengths.

2.2.3 Suspenders

The arch rib and the deck are connected at the panel points by suspenders. These suspenders are modelled as essentially rigid truss elements.

2.2.4 Treatment of Dead Load, Mass and Damping

The dead loads on the deck and the rib are assumed to be uniformly distributed on the horizontal projection. As mentioned previously, they are, as the mass, lumped at the panel points. Damping is assumed to be of the Rayleigh type, having critical damping ratios of 0.02 for the first two modes.

2.3 Loading

2.3.1 Live Load

In this study, when live load is considered, it is assumed to be uniformly distributed over the left half of the bridge deck. Its magnitude is computed according to the AASHTO specifications [5]. It consists of a uniform load of 0.64 kips/ft/lane plus a concentrated load of 18 kips to be placed at the most critical section. For convenience in using the computer program, the concentrated load was converted to a uniform load distributed over one half of the span on which the 0.64 kips/ft/lane was also applied. For the model, the number of lanes used in the load computation was equal to one half of the number of lanes for the bridge concerned.

2.3.2 Seismic Loading

Three ground motion inputs are used in the present study. They include the 1940 El Centro earthquake, and the B1 and B2 accelerograms which are two artificial earthquakes [6] of similar magnitude to the El Centro one. For dynamic analysis by the spectral method, the design response spectrum specified by AASHTO [5] is used.

2.4 Parameters

In this study, five sets of parameters are introduced: A, B, C, D and E, each complete by itself, so that the different sets can be used alternately. The first set, labeled A, is the basic dimensional parameters set. Second set B is mostly dimensionless. It is introduced to make the results more meaningful. Sets C, D and E are minor variations (involving two dimensionless parameters) of set B. They are used at different stages of the

investigation.

2.4.1 Dimensional Parameters: set A

The dimensional parameters are enumerated as follows:

1. L = length of bridge span
2. H = rise of bridge arch
3. A_r = cross-sectional area of arch rib
4. C_r = half depth of arch rib
5. I_r = moment of inertia of arch cross-section
6. A_d = cross-sectional area of bridge deck
7. C_d = Half depth of deck
8. I_d = moment of inertia of deck cross-section
9. N = number of panels
10. ξ = damping ratio
11. M = total mass per unit length
12. M_r = rib mass per unit length
13. E = Young' s modulus
14. A_s = cross-sectional area of bridge suspenders

2.4.2 Parameter set B

Some of the above listed parameters may be combined into dimensionless ones in order to provide greater insight into the behavior of the system. Set B is introduced to replace set A. It consists of the following parameters:

1. L = length of bridge span
2. ASTAR = total cross-sectional area of deck plus rib scaled by a "reference area", AA

$$ASTAR = \frac{A_d + A_r}{AA} \tag{2.1}$$

where

$$AA = \frac{M \times g \times L}{8 \times (\frac{H}{L}) \times F_a} \tag{2.2}$$

is equal to the rib dead load compressive force at the crown divided by a "reference allowable stress", F_a (set equal to 22 ksi herein).

3. ABAR = A_d/A_r = ratio of the cross-sectional area of the deck to the cross-sectional area of the rib

4. $$GSTAR = \frac{M \times g \times L^3}{E \times (I_d + I_r)} \tag{2.3}$$

This parameter is proportional to the dead load displacement divided by the span length L.

5. RHO = I_d/I_r = ratio of the moment of inertia of the deck to the moment of inertia of the rib

6. H/L = rise to span length ratio

7. M_r/M = rib mass to total mass ratio

8. C_r/R_r = ratio of rib half depth to R_r, rib section radius of gyration

9. C_d/R_d = ratio of deck half depth to R_d, deck section radius of gyration

10. N = number of panels

11. ξ = Damping ratio

12. M = total mass per unit length

13. E = Young' s modulus (E = 29000 ksi)

14. A_s = cross-sectional area of the bridge suspenders

As mentioned earlier, the parameters of set B are mostly dimensionless. The reason for replacing set A by set B is because the results presented in terms of dimensionless parameters are generally more meaningful. Also, according to the theory of dimensional analysis, the total number of dimensionless parameters for the problem may be reduced from the dimensional set, i.e, 14, by three; three being the basic dimensions of the problem, i.e., length, force (or mass) and time. In the set presented here, effectively, the number of parameters can be regarded as reduced by two. The "time" dimension is not made dimensionless because it seems unwieldy to scale the seismic motion in terms of dimensionless time. In set B, one may eliminate M and E as parameters when dimensionless responses, such as stress amplification factors and displacement ratios, are considered. The cross-sectional area of the suspenders A_s may also be eliminated as a parameter by making the suspenders essentially rigid members.

2.4.3 Sets C, D and E

Sets C, D and E are each obtained by replacing two of the dimensionless parameters of set B by two different ones.

1. Set C is obtained by replacing $ASTAR$ and C_r/R_r, of set B, by $ALPHA$ and D_d/D_r, where

$$ALPHA = \frac{M \times g \times L^2}{E \times \sqrt{I_r \times A_r}} \tag{2.4}$$

or, in terms of set B parameters,

$$ALPHA = \sqrt{\frac{8 \times F_a \times (\frac{H}{L}) \times GSTAR \times (1+ABAR) \times (1+RHO)}{E \times ASTAR}} \tag{2.5}$$

and

$$\frac{D_d}{D_r} = \sqrt{\frac{RHO}{ABAR}} \times \left(\frac{\frac{C_d}{R}_d}{\frac{C_r}{R}_r} \right) \tag{2.6}$$

Set C parameters were used to classify the samples of existing tied arch bridges into three types, as discussed in section 2.6.2, and in Chapter 3, when examining the seismic response of the three bridge types.

2. Set D is obtained from set B by replacing *ASTAR* and *GSTAR* by $(L/R)_c$ and *GAMMA* respectively, where

$$(\frac{L}{R})_c = \frac{L}{\sqrt{\frac{(I_d+I_r)}{A_r}}} \tag{2.7}$$

or

$$(\frac{L}{R})_c = \sqrt{\frac{ASTAR \times GSTAR \times E}{8 \times F_a \times (\frac{H}{L}) \times (1+ABAR)}} \tag{2.8}$$

and

$$GAMMA = GSTAR \times (1+RHO) \tag{2.9}$$

Set D parameters are introduced in Chapter 5, and used to compare the seismic response of the tied type bridges with the deck type bridges.

3. Set E is obtained from set B by replacing *ASTAR* and *GSTAR* by *V* and *ALPHA* respectively, where *V* is the volume of deck and rib members. It may be expressed as a function of set B parameters as:

$$V = \frac{M \times g \times L^2 \times ASTAR \times (ABAR + \frac{L_R}{L})}{8 \times F_a \times (\frac{H}{L}) \times (1 + ABAR)} \tag{2.10}$$

where L_R, the curved length of the arch rib, is a function of *H/L* and *L*. *ALPHA* is as given by Equation 2.4. Set E was used to generate three types of bridges to be discussed in section 2.6.3 in order to investigate whether three bridges, with the same length and amount of structural material, but of different types, would behave differently, especially under seismic loading.

It is emphasized again that each of the five sets is complete in the sense that it uniquely defines the problem; i.e., a given bridge may be uniquely defined by any one of the sets.

2.5 Response Quantities

The response quantities considered in the present study are:

1. The maximum live load stress, f_{LL}
2. The maximum dead load stress, f_{DL}
3. The maximum earthquake stress, f_{EQ}
4. The maximum combined dead load and earthquake stresses: $f_{DL}+f_{EQ}$
5. The maximum combined dead load and live load stresses: $f_{DL}+f_{LL}$

6. The stress amplification factor, which is the ratio of seismic plus dead load stress to dead load stress: *BSMAXX*, for the deck straight beam elements, and *SMAXX* for the rib curved beam elements
7. The nodal vertical displacements, scaled by the span length.

2.6 Samples of Existing Bridges

2.6.1 Properties of Actual Bridges

Seven actual bridges are considered: the North Fork Stillaguamish River Bridge, the Leavenworth Centennial Bridge, the Fort Duquesne Bridge, the Fort Henry Bridge, the Glenfield Bridge, the Fort Pitt Bridge, and the West End-North Side Bridge. The parameters of concern for these bridges were computed from data obtained from the Steel Design Handbook [8]. The dimensional properties (set A) of the above bridges are presented in Table 2.1. The parameters of set B are presented in Table 2.2. Table 2.3 lists the parameters of sets C, D and E that replace the parameters of set B.

2.6.2 Definition of Three Bridge Types

When examining the numerical values of the parameters of set C, it was noticed that the bridges may be classified into three groups: heavy rib-light deck, designated as type A, light rib-heavy deck, designated as type B, and medium rib-medium deck, designated as type C. In Table 2.4 are shown the classification of the seven sample bridges and the associated values of the parameters. Table 2.5 lists the definitions of the "representative values" for each bridge type. The three sets of representative values thus defined are used as reference parameter sets to generate three bridge sets with the same length, amount of structural

material, and total weight, corresponding to each type. This is described in the next section.

2.6.3 Generated Bridges

In the previous section, three relatively distinct types of tied arch bridges are defined. It is natural to investigate for a given bridge belonging to a given type, whether it would behave differently, particularly with reference to seismic response, if it were "designed" as the other types. For this consideration, the following procedure was followed.

1. A representative bridge of each type is selected: Fort Henry (type A), Glennfield (type B), and Leavenworth (type C).
2. The length, volume (of structural material) and mass of each of these real bridges, along with the representative values chosen for each bridge type, are used to generate three bridges, with the same length, volume and mass, but with the other parameters pertaining to the different types in accordance with the definition. The question to be answered is whether the three bridges of different types, would respond differently under live load, dead load, and particularly seismic excitation. This is investigated in chapter three. In the remainder of this section, it is shown how three bridge types are generated.

For each representative or prototype bridge the volume of the structural material is computed as:

$$V = L \times A_d + L_r \times A_r \tag{2.11}$$

From the fixed volume of each representative bridge, two additional bridges are generated, using their representative values of the parameters. The parameters that define each bridge that is generated are computed as follows:

$$A_r = \frac{V}{L \times (ABAR^* + \frac{L_r}{L})} \tag{2.12}$$

where $ABAR^*$ is taken from the representative values defining each bridge type. (In the expressions given in this section, quantities with a star superscript represent representative values as listed in Table 2.5; those without, pertain to properties of the prototype bridge.)

$$I_r = \frac{(M \times g)^2 \times L^4}{E^2 \times A_r \times ALPHA^{*2}} \tag{2.13}$$

where Mg is the total dead load per unit length for the prototype bridge, A_r is the rib cross-sectional area as computed above and $ALPHA^*$ is the ratio of dead load factor to slenderness ratio of the arch rib, taken from the representative value parameter sets defining each bridge type. The value of the parameter $GAMMA$ may be computed from

$$GAMMA = ALPHA^* \times \frac{L}{R_r} \tag{2.14}$$

in which

$$R_r = \sqrt{\frac{I_r}{A_r}} \tag{2.15}$$

using the central value of (M_r/M), the rib mass is equal to

$$M_r = \left(\frac{M_r}{M}\right)^* \times M \tag{2.16}$$

where $(M_r/M)^*$ is the representative value of the parameter for the bridge type. Similarly,

$$RHO = \frac{I_d}{I_r} = ABAR^* \left(\frac{D_d}{D_r}\right)^{*2} \left(\frac{\left(\frac{C_r}{R_r}\right)^*}{\left(\frac{C_d}{R_d}\right)^*} \right)^2 \tag{2.17}$$

The main parameters for the three bridge types and the other two bridge types generated from each of them, are shown in Table 2.6. Each generated bridge is denoted by the letter corresponding to its own type, preceded by the letter corresponding to the type it is generated from. For example, bridge a/b is a bridge of type B generated from a type A bridge.The parameter sets of these generated bridges are used in section 3.4.4 when computing a "structural zone factor".

Table 2.1 Parameters of Sample Real Bridges (Set A)

Bridge	L (ft)	H (ft)	A_r (ft^2)	C_r (ft)	I_r (ft^4)	A_d (ft^2)	C_d (ft)	I_d (ft4)	N	W (kip/ ft)	W_r (kip/ ft)
Leavenworth	420.0	80.0	0.69	1.46	0.86	0.83	3.08	4.65	13	3.35	0.493
North Fork	278.6	51.0	0.51	1.06	0.36	0.72	2.13	2.15	11	3.00	0.342
West End-North	778.0	151.0	2.62	14.68	412.60	1.74	1.66	1.61	28	7.57	3.475
Fort Pitt	750.0	122.2	4.47	2.68	17.42	4.88	14.65	765.28	30	18.43	2.740
Glennfield	750.0	124.4	1.92	2.24	7.17	3.08	6.27	93.06	15	13.57	1.280
Fort Henry	577.5	110.9	1.92	4.56	25.18	1.37	1.45	1.08	15	7.46	1.710
Fort Duquesne	423.0	64.6	2.12	2.15	5.16	2.37	13.43	328.75	18	14.99	1.080

Table 2.2 Parameters of Sample Real Bridges (Set B)

Bridge	L (ft)	ASTAR	ABAR	GSTAR	RHO	H/L	M_r/M	$(C/R)_r$	$(C/R)_d$	N
Leavenworth	420.0	5.26	1.20	10.76	5.410	0.192	0.147	1.31	1.30	13
North Fork	278.6	6.80	1.41	6.23	5.970	0.182	0.114	1.26	1.23	11
West End-North	778.0	3.61	0.664	1.99	0.004	0.192	0.284	1.17	1.73	28
Fort Pitt	750.0	2.76	1.09	2.38	43.930	0.161	0.149	1.36	1.17	30
Glennfield	750.0	2.07	1.60	13.64	13.000	0.167	0.094	1.16	1.14	15
Fort Henry	577.5	3.72	0.71	13.42	0.043	0.192	0.229	1.26	1.63	15
Fort Duquesne	423.0	2.76	1.12	0.82	63.710	0.154	0.072	1.38	1.14	18

Table 2.3 Alternative Parameters of Sample Real Bridges (Sets C, D and E)

Bridge	ALPHA (set C)	D_d/D_r (Set C)	$(L/R)_c$ (Set D)	GAMMA (Set D)	V (ft^3) (Set E)
Leavenworth	0.18	2.11	148.59	69.41	664.39
North Fork	0.13	2.01	126.15	43.46	NA
West End-North	0.03	0.11	60.87	2.07	NA
Fort Pitt	0.28	5.47	56.72	106.85	NA
Glennfield	0.49	2.80	103.51	191.10	3874.80
Fort Henry	0.09	0.32	158.29	13.67	2000.95
Fort Duquesne	0.19	6.25	33.80	52.69	NA

Table 2.4 Classification of Bridge Types

Bridge	Type	ALPHA	D_d/D_r	ABAR	RHO
Fort Henry	A	0.09	0.32	0.71	0.043
West End-North	A	0.03	0.11	0.66	0.004
Glennfield	B	0.49	2.80	1.60	13.000
Fort Pitt	B	0.28	5.47	1.09	43.930
Fort Duquesne	B	0.19	6.25	1.12	63.710
Leavenworth	C	0.18	2.11	1.20	5.410
North Fork	C	0.13	2.01	1.41	5.970

Table 2.5 Representative Parameter Values of Prototyppe Bridges

Bridge type	ALPHA	D_d/D_r	ABAR	$(C/R)_r$	$(C/R)_d$	M_r/M
A	0.05	0.21	0.688	1.20	1.68	0.26
B	0.33	4.91	1.270	1.30	1.15	0.10
C	0.15	2.13	1.300	1.28	1.26	0.13

Table 2.6 Basic Parameters of Generated Bridges

Bridge type	ALPHA	M_r/M	$(C/R)_r$	$(C/R)_d$	ABAR	I_d/I_r	Gamma	M_r
Bridges generated from type A bridge								
a/a	0.05	0.26	1.20	1.68	0.688	0.01548	4.7194	1.9396
a/b	0.30	0.10	1.30	1.15	1.270	39.12530	128.0204	0.7460
a/c	0.15	0.13	1.28	1.26	1.300	6.08670	31.6046	0.9698
Bridges generated from type B bridge								
b/a	0.05	0.26	1.20	1.68	0.688	0.01548	2.9857	3.5282
b/b	0.30	0.10	1.30	1.15	1.270	39.1253	80.944	1.3570
b/c	0.15	0.13	1.28	1.26	1.300	6.0867	19.9819	1.7641
Bridges generated from type C bridge								
c/a	0.05	0.26	1.20	1.68	0.688	0.01548	6.6023	0.8710
c/b	0.30	0.10	1.30	1.15	1.270	39.12530	179.0790	0.3350
c/c	0.15	0.13	1.28	1.26	1.300	6.08670	44.2074	0.4355

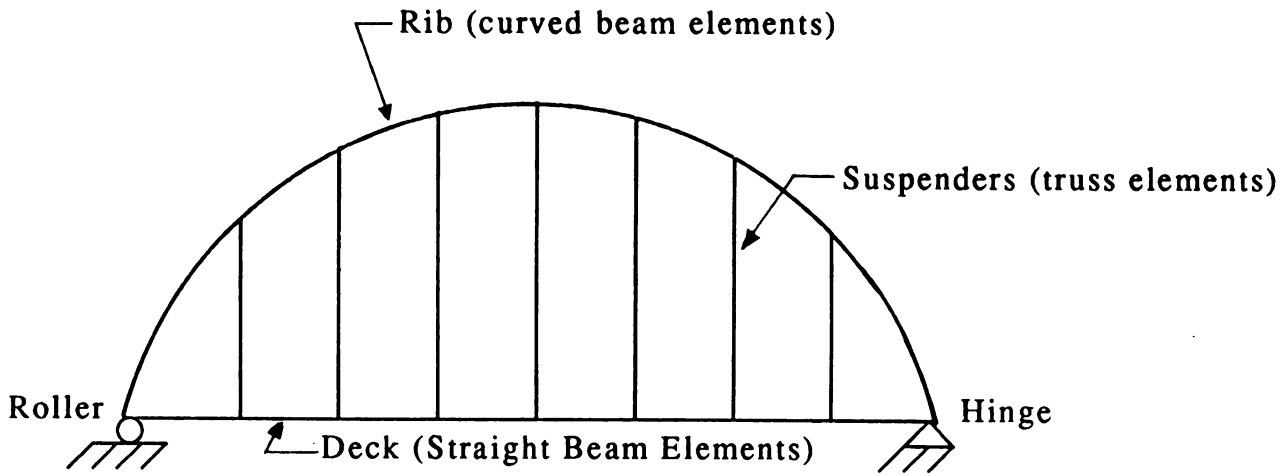

Figure 2.1 Tied Arch Bridge Model

3. SEISMIC RESPONSE

3.1 General

In this chapter, the seismic response of tied arch bridges is discussed. Parameter set D is used as the reference set in section 3.3.1, when discussing the natural frequencies and the normal modes. Parameter set C is the reference parameter set for the remainder of the chapter. In the first part, the method of analysis is discussed, including the equation of motion, the types of analyses used to compute the response quantities, and the computer program used in computer modelling. In the second part, the dynamic characteristics (natural frequencies and normal modes) of a tied bridge are presented. In the third part, the seismic response is presented by comparing the bridge response to different ground motion inputs (design spectrum and time history). Finally, in the last section of this chapter, the importance of earthquake loading relative to live load is investigated by introducing a structural zone factor that compares the responses under dead plus live load and under dead plus earthquake load.

3.2 Method of Analysis

3.2.1 Equation of Motion

The equation of motion of the bridge subjected to earthquake

excitations may be expressed as:

$$[m]\{\ddot{u}\} + [c]\{\dot{u}\} + \{r\} = -[m]\{\ddot{u}_g\} \tag{3.1}$$

where m is the lumped mass matrix, c is the damping matrix of Rayleigh type, r is the resistance vector, u is the displacement vector with respect to the ground, and the dot superscripts denote derivatives with respect to time. $\ddot{u}_g$ is the ground acceleration vector. The derivation of the equation of motion may be found in Reference [9]. It may be noted that if linearly elastic behavior is presumed, {r} = [k]{u}, in which [k] is the linear stiffness matrix, and equation (3.1) becomes:

$$[m]\{\ddot{u}\} + [c]\{\dot{u}\} + [k]\{u\} = -[m]\{\ddot{u}_g\} \tag{3.2}$$

This equation may be found in most textbooks on structural dynamics (e.g. [10]) and is used for most of this thesis.

3.2.2 Time History Analysis

The equation of motion is integrated over the time domain by the well known Newmark β method, with β equal to 1/4 in the numerical integration. When computing the dynamic response, a time step equal to 0.02 times the fundamental period was used. (A detailed description of the method of solution is given in Reference [9]. In the solution process, the dead load is applied first and the static response is computed. Then the structure is subjected to seismic input and the dynamic response computed. For geometrically nonlinear analysis, the static load is applied in ten equal increments and then the seismic loading applied. The Newton-Raphson

method is used to compute both the static and the dynamic response. In the present study, the results presented were obtained using linear analysis after it was first established, as expected, for the tied arch bridges, the effects of geometric nonlinearity was negligible.

3.2.3 Spectral Analysis

The response quantities considered are computed by the SRSS (Square Root of the Sum of the Squares) method. Other methods, such as the CQC (Complete Quadratic Combination) method or the "Ten Percent Method" could be used. However, since for the system considered, the frequencies are relatively well separated and the damping is small, the choice of the SRSS method is justified. Ten normal modes were found to be sufficient to give satisfactory accuracy. The stress corresponding to each mode is computed as the sum of the absolute values of the axial and bending stresses corresponding to that particular mode:

$$s_i = \left|\frac{P_i}{A}\right| + \left|\frac{M_i}{S}\right| \tag{3.3}$$

where P_i and M_i are the modal axial force and bending moment, respectively, corresponding to mode i, A is the cross-sectional area, and S is the section modulus. The SRSS of the modal stresses is computed to obtain the absolute maximum stresses at each node.

A second and more accurate method to obtain the maximum stresses is by considering two different points at a given cross-section (top and bottom fibers of the section). The two points are symmetric about the y-axis. From strength of materials, the stresses at these two points of the cross-

section considered are obtained by adding or subtracting the bending stress from the axial stress:

$$S_{t,i} = \left| \frac{P_i}{A} + \frac{M_i}{S} \right| \tag{3.4.a}$$

$$S_{b,i} = \left| \frac{P_i}{A} - \frac{M_i}{S} \right| \tag{3.4.b}$$

in which the subscripts t and b denote, respectively, the top and bottom fiber of the cross-section. The SRSS method is used to obtain the maximum stress for each of the two points at the cross-section, and the larger of the two would be reported as the maximum stress for the section.

The second method gives a better estimation of the value of the stresses. The first gives an upper bound of the second. The difference, however, is not large, on the order of five percent. Equation 3.3 was used in obtaining the numerical results for Chapters three and five and Equation 3.4 for Chapter four.

3.2.4 Computer Program Used

When conducting the research, a modified version of the NOALIST program [11] was used to compute the response quantities. The modifications included the following:

1. Originally, the program was written for deck type arch bridges. It was modified to accept specifications for tied arch bridges. The modifications mainly were concerned with automatic generation of data with the altered geometry and support conditions of the bridge.
2. The program was also modified to include the response (maximum stresses and maximum amplification factors) of straight beam elements that

represent the deck.

3. The time history program was modified to include computations of stresses and displacements under live load. These computations are incorporated directly in the program so that the live load, dead load and seismic load analyses may be obtained in one computer run.

4. The program now includes outputs of the axial and bending stresses as fractions of the total stress.

3.3 Natural Frequencies and Normal Modes

It is of interest to examine the dynamic characteristics of tied arch bridges in order to better understand their response to dynamic excitations. In the first part of this section, the natural frequencies and normal modes of a tied arch bridge are presented. In the second part, the effects of the axial and bending stiffnesses on the fundamental frequency of a type A bridge (bridge a/a) are investigated.

3.3.1 Natural Frequencies and Normal Modes of a Tied Arch Bridge

The shapes of the first ten modes of a T-Type bridge and their corresponding frequencies are shown in Figures 3.1.a- 3.1.j. The bridge for which the mode shapes are shown has the following parameters: L = 750ft, H/L = 0.175, M = 4.8 kip/ft, $ABAR$ = 0.688, RHO = 0.0, $GAMMA$ = 5.25, $(L/R)_c$ = 200.0, C_r/R_r = 1.275, and C_d/R_d = 1.275. The parameter RHO is null, meaning that the bridge deck is represented by a truss member with no bending stiffness.The first mode is a full wave shape of the arch and the deck. the second mode shows a one and a half wave vertical motion of the rib and deck. The third mode is a two wave shape of the rib and deck. The fourth mode indicates significant axial deformations of the rib. The deck

has some waves which are not about the bridge axis, which would mean that the motion is controlled by both bending and axial forces. The fifth mode is a two and a half wave motion of the arch and deck. The sixth mode is a three wave motion of the rib and deck. The seventh mode is a three and a half wave motion of the rib and deck. The eight mode, like the fourth mode, suggests a significant axial deformation component but with a larger number of waves due to bending. The ninth and tenth modes seem nondescript. The modes are mainly controlled by bending, except for the fourth and eight mode, especially in the case of the rib.

3.3.2 Effect of Stiffness on the Fundamental Frequency

The bridge considered here is of type a (heavy rib, light deck). Its design characteristics are taken from the existing Fort Henry bridge and are shown in Table 2.5. $ALPHA$ = 0.05, M_r/M = 0.26, (C_r/R_r) = 1.2, (C_d/R_d) = 1.68, $ABAR$ = 0.688, RHO = 0.01548, D_d/D_r = 0.21, M_r = 1.9396 kip/ft. The fundamental frequency is independent of the axial stiffness; it does not change with increasing total area or deck plus rib. Figure 3.2 shows the fundamental frequency when RHO is varied from 0.0 to 1.0, while all other parameters are kept constant. In Figure 3.2.a, the bending stiffness of the rib is constant, but the total bending stiffness is increased. In Figure 3.2.b, the total bending stiffness is constant, but the individual bending stiffnesses of the deck and the rib are changing. Figure 3.2 shows that the fundamental frequency varies very little with RHO when the total bending stiffness is constant. However, it increases with RHO when the total stiffness increases. Essentially, the fundamental frequency seems to be dependent on the total bending stiffness of the bridge, and not on the individual stiffnesses of the arch and the deck.

3.4 Seismic Response

3.4.1 Ground Motions and Design Spectrum

The actual 1940 El Centro earthquake and the B1 an B2 artificial earthquakes mentioned in section 2.3.2 are used in time history analysis as ground motion input with equal motion for both supports in both the vertical and horizontal direction. The North-South component of El Centro is used for longitudinal motion input and its vertical component is used for vertical motion input. The acceleration of the B1 and B2 earthquakes are scaled so that they have the same maximum acceleration as the North-South component of El Centro. Their vertical acceleration is taken to be 75 percent of their horizontal one. The AASHTO response spectrum [5] is used for spectral analysis. It is summarized as follows. The spectral acceleration, SA, in terms of g is given by:

$$SA = \frac{1.2 \times A \times S}{T_i^{2/3}} \tag{3.5}$$

for $T_i < 4.0$ sec., and

$$SA = \frac{3.0 \times A \times S}{T_i^{4/3}} < 2.5 \times A \tag{3.6}$$

for $T_i > 4.0$ sec., where T_i is the ith natural period, A is the ("bedrock") acceleration in g and S is a site (soil) coefficient. In this analysis, A and S are taken to correspond to the "strongest" ground motion and soil, i.e., A = 0.4, and S = 1.0.

3.4.2 Comparison of results

In this section, the response computed by the spectral solution is compared with the responses computed by the time history solutions when the structure is subjected to the ground motions mentioned above. The response quantities considered here are the stress amplification factor: maximum dead load plus seismic stress/maximum dead load stress, *BSMAXX* for the straight beam elements; *SMAXX* for the curved beam elements; and the ratio of nodal displacement to span length. These quantities are computed for the representative bridge of each type: a/a (heavy rib, light tie), b/b (light rib, heavy tie), and c/c (medium rib, medium tie). The values of the time history response quantities are averaged and compared to the spectral values. Table 3.1 shows the stress amplification factors.The spectral value compares very well with the average of the three ground motions. Table 3.2 shows the displacement ratios for the three time history ground motions, their average value, and the spectral value. The spectral value of the displacement ratio is also close to the average of the three ground motions. This suggests that the response spectra, recommended by the AASHTO [5], predicts well the response of this bridge type to seismic excitations.

3.5 Relative Importance in Design

3.5.1 General

When studying the response of a bridge structure to earthquake excitations, for a proper perspective, it is important to first investigate its behavior under static loading. In this section, the distribution of the stresses and of the stress resultants under dead and live loads are first

examined. Then the stresses under the load combinations normally considered in design, i.e., dead load plus live load and dead load plus earthquake load, are compared by introducing a structural zone factor, denoted by Z_{st}, at which the effect of live load plus dead load and that of dead load plus earthquake load are equal.

3.5.2 Dead and Live Load Response

The bridge considered in this section is the representative bridge of Type A (bridge a/a: Heavy Rib-Light Deck). Figure 3.3 shows the distribution of the stress resultants in the bridge members under dead load. Figure 3.4 shows the stress distribution in the bridge members under dead load. The internal forces (stress resultants) are much higher in the arch rib than in the deck. This is understandable since, in the case of this bridge (heavy rib, light tie), the rib is much stiffer than the deck (RHO = 0.01548). However, the stresses in the arch and in the deck are close. The rib has higher axial forces and bending moments than the tie. It also has larger area and moment of inertia. The differences tend to vanish when the stress is computed.

From structural theory, it is known that the bending moment on a parabolic arch vanishes when the loading on the horizontal projection is uniform. In the case of this bridge, eight panels are used for a length of 577.5 ft, and the mass is lumped at the panel points. The load distribution is not exactly uniform, which explains the relatively large bending moments in the arch rib.

Figure 3.5 shows the stress resultants distribution in the arch rib and the bridge deck under live load. The anti-symmetry of the bending moment in the arch is due to the fact that only the left half of the bridge is loaded.

The axial forces in the rib and tie are close, although the moments in the arch are much higher than in the tie (compared to the dead load case). That explains why the difference in the stresses is bigger than in the case of the dead load. At the midspan, where the internal forces are very close in the arch and in the tie, the stresses are equal. Figure 3.6 shows the distribution of the live load stresses in the deck and the rib.

3.5.3 ($f_{DL}+f_{LL}$) versus ($f_{DL}+f_{EQ}$), and the "Structural Zone Factor"

In this section, a structural zone factor is computed and discussed in order to investigate which load combination: dead load plus live load or dead load plus seismic load governs the design of each one of the bridge types. The zone factor is computed by making the dead load plus live load stress equal to the dead load plus a fraction (= Z_{st}) of the earthquake stress, the dead load and earthquake stresses being reduced by 33% to account for the usual increase in allowable stress of 1/3 in the case of seismic design. Thus, one may write:

$$f_{DL}+f_{LL} = \frac{f_{DL}+Z_{st}\times f_{EQ}}{1.33} \tag{3.7}$$

from which:

$$Z_{st} = \frac{0.33f_{DL}+1.33f_{LL}}{f_{EQ}} \tag{3.8}$$

where f_{LL} is the live load stress, f_{DL} is the dead load stress, f_{EQ} is the earthquake stress and Z_{st} is the "structural zone factor".

When Z_{st} is equal to unity, the live load effect is just equal to the effect of an earthquake of the intensity considered here (i.e., AASHTO A = 0.4, S = 1.0). Table 3.3 shows the maximum live load, dead load, and seismic load stresses and the structural zone factor as computed above for the prototype bridge of each type (a/a, b/b, and c/c bridges), both for the tie and for the arch rib. For more exploratory data, Table 3.4 shows the "structural zone factor" for the three bridge types and for the generated bridges of the other two types corresponding to them. It is noticed, from Table 3.4, that for bridge types b and c, Z_{st} is always greater than 1.0 for the curved beam elements of the arch rib. This would mean that if these bridges are built at a site with smaller seismicity than considered here, live load effects would govern the design.

It is also noticed that for type a, Z_{st} is always less than 1.0, for the straight beam elements of the bridge tie. The "structural zone factor" can be compared to the site zone factor z_s which may be computed as follows:

$$z_s = \frac{(A)_{site} \times S_{site}}{(A \times S)_{used}} \tag{3.9}$$

in which A_{site} and S_{site} are, respectively, the ground acceleration and soil factor for the site under consideration and $(A \times S)_{used} = (0.4 \times 1.0)$ as used in obtaining the results presented. If the "structural zone factor" is smaller than the site zone factor, then earthquake loading would govern the design.

Table 3.1 Comparison of Time History Solutions (Stress Amplification Factor) with Spectral Solutions for Three Bridge Types

	BSMAXX	M, I	SMAXX	M, I
Type A bridge				
El Centro	1.78	8, 1	1.85	5, 1
B1	1.80	5, 1	2.11	4, 2
B2	1.83	8, 1	2.31	7, 2
Average	1.80		2.09	
Spectral	1.83	8, 1	2.19	7, 2
Type B bridge				
El Centro	1.73	8, 2	1.30	7, 2
B1	1.56	8, 2	1.35	5, 1
B2	1.98	5, 1	1.71	6, 2
Average	1.76		1.45	
Spectral	1.69	8, 2	1.39	7, 1
Type C bridge				
El Centro	2.16	8, 1	1.47	6, 2
B1	3.04	1, 2	2.07	3, 1
B2	3.20	8, 1	1.86	3, 1
Average	2.80		1.80	
Spectral	2.99	8, 1	1.68	7, 2

Table 3.2 Comparison of Time History Solutions with Spectral Solution (Displacement/Span length)

	Deck left quarter point	Deck midspan	Deck right quarter point	Arch left quarter point	Arch crown	Arch right quarter point
Type A bridge						
El Centro	0.001060	0.001650	0.001010	0.000973	0.001510	0.000925
B1	0.001150	0.002030	0.001080	0.001070	0.001880	0.001010
B2	0.001230	0.001590	0.001360	0.001120	0.001460	0.001250
Average	0.001150	0.001760	0.001150	0.001050	0.001620	0.001060
Spectral	0.001168	0.001659	0.001146	0.001077	0.001512	0.001054
Type B bridge						
El Centro	0.001630	0.002300	0.001720	0.001410	0.002090	0.001510
B1	0.001770	0.002710	0.001840	0.001560	0.002420	0.001630
B2	0.002190	0.003320	0.002340	0.001900	0.002980	0.002040
Average	0.001860	0.002780	0.001970	0.001620	0.002500	0.001730
Spectral	0.001839	0.002743	0.001946	0.001613	0.002450	0.001721
Type C bridge						
El Centro	0.000752	0.001000	0.000821	0.000696	0.000936	0.000759
B1	0.001260	0.001060	0.001020	0.001180	0.001000	0.000949
B2	0.001150	0.001090	0.001090	0.001070	0.001010	0.001020
Average	0.001050	0.001050	0.000977	0.000982	0.000982	0.000909
Spectral	0.000936	0.001139	0.000921	0.000872	0.001064	0.000858

Table 3.3 Maximum Stresses and Structural Zone Factor

Bridge deck	live load stress(ksi)	Dead load stress(ksi)	Seismic stress(ksi)	Z_{st}
Bridge deck				
Type a	2.030	16.060	12.180	0.660
Type b	5.130	30.820	17.060	0.996
Type c	6.430	10.070	14.520	0.820
Bridge arch rib				
Type a	5.301	15.600	17.700	0.690
Type b	3.620	43.200	16.650	1.140
Type c	4.420	19.410	11.820	1.040

Table 3.4 Structural Zone Factor for Generated Bridges

Type A			
	a/a	a/b	a/c
Deck	0.66	0.73	0.78
Arch	0.69	1.00	1.20
Type B			
	b/a	b/b	b/c
Deck	0.80	1.00	1.04
Arch	1.05	1.14	1.21
Type C			
	c/a	c/b	c/c
Deck	0.62	0.74	0.82
Arch	0.89	1.05	1.04

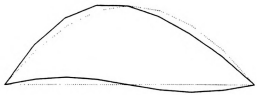

(a) First Mode, Natural Frequency = 0.52041 (HZ)

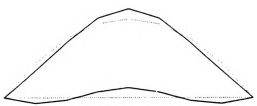

(b) second Mode, Natural Frequency = 1.12356 (HZ)

Figure 3.1 First Ten Modes of A Tied Arch Bridge (continued)

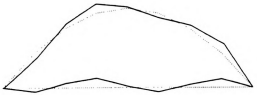

(c) Third Mode, Natural Frequency = 2.09616 (HZ)

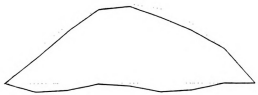

(d) Fourth Mode, Natural Frequency = 2.15025 (HZ)

Figure 3.1 First Ten Modes of A Tied Arch Bridge (continued)

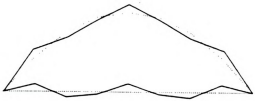

(e) Fifth Mode, Natural Frequency = 3.26269 (HZ)

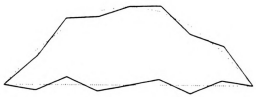

(f) sixth Mode, Natural Frequency = 4.44230 (HZ)

Figure 3.1 First Ten Modes of A Tied Arch Bridge (continued)

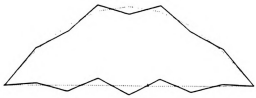

(g) Seventh Mode, Natural Frequency = 5.47949 (HZ)

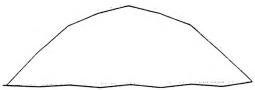

(h) Eight Mode, Natural Frequency = 5.76301 (HZ)

Figure 3.1 First Ten Modes of A Tied Arch Bridge (continued)

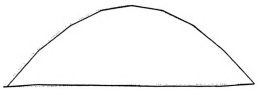

(i) Ninth Mode, Natural Frequency = 11.51545 (HZ)

(j) Tenth Mode, Natural Frequency = 15.99208 (HZ)

Figure 3.1 First Ten Modes of A Tied Arch Bridge (continued)

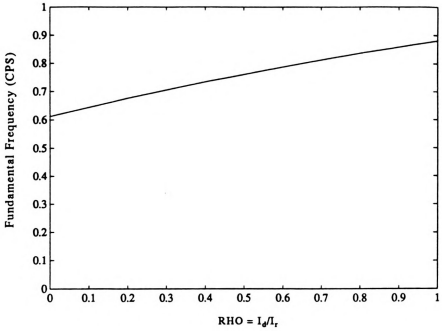

(a) I_r = constant

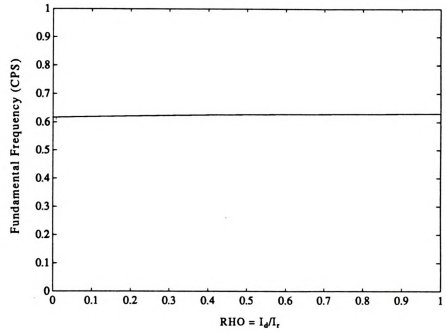

(b) $I_r + I_d$ = constant

Figure 3.2 Effect of RHO on Fundamental Frequency

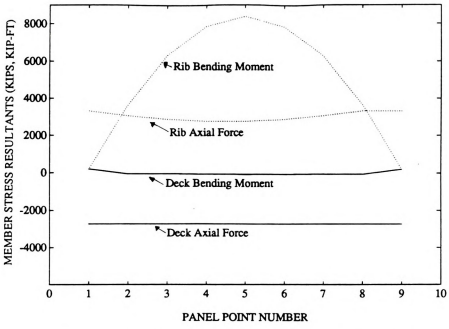

Figure 3.3 Distribution of Stress Resultants Due to Dead Load

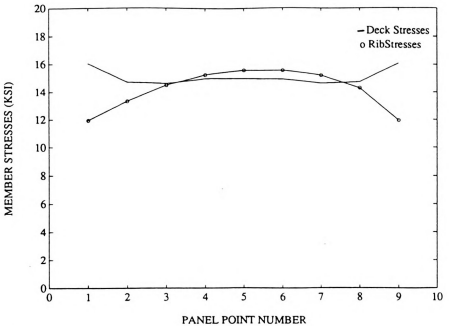

Figure 3.4 Distribution of Maximum Stress Due to Dead Load

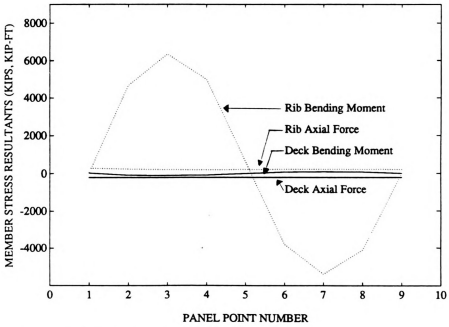

Figure 3.5 Distribution of Stress Resultants Due to Live Load

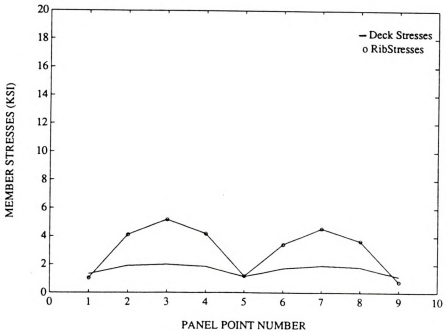

Figure 3.6 Distribution of Maximum Stress Due to Live Load

4. "OPTIMAL DESIGN"

4.1 Introduction

As noted in the sample real bridges presented in Chapter 2, there are widely different material distributions between rib and deck structural members. It is interesting to inquire whether there is an "optimal" distribution of structural material between the rib and the deck, so far as earthquake effects are concerned. An "optimal value" may be defined, based on ABAR (the ratio of the cross-sectional area of the rib to that of the deck) as follows: with other parameters fixed, the "optimal value" of ABAR is taken to be that value at which the maximum dead load plus earthquake load stress in the rib and that in the deck are equal. It will be shown that a deviation from that value would lead to a higher stress in either the rib or the deck.

4.2 Parameters

For the purposes of this chapter, parameter set B is used. The parameters that are varied are:

1. *L*, span length. Three values: 200.0 ft, 400.0 ft and 800.0 ft are considered.

2. *ASTAR*, as defined previously, the sum of the cross-sectional areas of the rib and the deck scaled by a reference area, (see equation 2.1). Three

values: 1.00, 2.00, and 3.00 are considered.

3. *GSTAR*, the "dead load factor" (see Equation 2.3). It is a measure of the total structural stiffness. Three values: 2.0, 5.0 and 10.0 are considered.

In addition, in this chapter *RHO* (the deck bending stiffness to rib bending stiffness ratio) is assumed to be equal to the squared value of *ABAR*. The assumption is based on the following derivation:

A box cross-sectional area (of depth D and thickness t) is assumed for both the rib and the deck (the depth and thickness are not necessarily equal for the deck and the rib). The ratio *RHO* can be written as:

$$RHO = \frac{A_d \times R_d^2}{A_r \times R_r^2} \tag{4.1}$$

The radius of gyration of the rib may be reasonably assumed to be proportional to the depth of its cross-section:

$$R_r = \alpha_r \times D_r \tag{4.2}$$

Also, the radius of gyration of the deck is assumed to be proportional to the depth of its cross-section:

$$R_d = \alpha_d \times D_d \tag{4.3}$$

Assuming further, $\alpha_d = \alpha_r$, and substituting 4.2 and 4.3 in 4.1, gives:

$$RHO = \frac{A_d}{A_r} \times \left(\frac{D_d}{D_r}\right)^2 \tag{4.4}$$

Assuming that the cross-sectional area to be proportional to the depth times the thickness, and the thickness to be proportional to the depth; then

$$A \propto D \times t = p \times D^2 \tag{4.5}$$

in which, p is a constant of proportionality.

From 4.4 and 4.5, and a final assumption that the value of p in equation 4.5 for the rib and deck sections are equal, one arrives at the relation that

$$RHO = (ABAR)^2 \tag{4.6}$$

The above assumption seems reasonable. When the proportions of the material in the rib and in the deck vary, the proportions of the bending stiffnesses vary accordingly.

The remaining parameters are fixed in value, as shown below:

H/L = 0.175

M_r/M = 0.265

C_r/R_r = 1.275

C_d/R_d = 1.275

Mg = 4.80 kips/ft

4.3 Results

4.3.1 Effect of Parametric Variations on the Fundamental Frequency

Figures 4.1 show the fundamental frequency as a function of *ABAR* for the different values of *ASTAR* and *GSTAR*, and span lengths. As expected, the curves are rather flat. This is understandable since, for each of these plots, *GSTAR* is constant,i.e, the total structural stiffness is constant. In the remainder of this section, the effect of *L*, *ASTAR* and *GSTAR* on the fundamental frequency, while *ABAR* is constant, are discussed. Table 4.1 shows the values of the fundamental frequency for the parameters that are varied, for a constant value of *ABAR* of 1.0. The table shows that:

1. The fundamental frequency decreases with increasing length. This is expected; a longer bridge has a longer fundamental period, all other parameters being equal.

2. When ASTAR increases, the fundamental frequency increases for a GSTAR value of 2.0, but remains unchanged for the higher GSTAR values of 5.0 and 10.0. When GSTAR is higher, the structure is more flexible in bending and increasing the areas of rib and deck, thus increasing the "axial stiffness", does not effect its natural frequency significantly. For the structure stiffer in bending (low value of *GSTAR*), an increase in the fundamental frequency is noticed with increasing values of *ASTAR* (here, *ABAR* is constant and *RHO* is constant). When ASTAR is increased, both cross-sectional areas of the deck and the arch increase. From the previous chapter, when the area of the rib is constant, the fundamental frequency is hardly affected, although the total area is increasing (and therefore the area of the deck is increasing). It appears then, that in the cases of arch

structures with larger bending stiffness, the fundamental frequency would be affected more by the cross-sectional area of the rib than that of the deck.
3. When *ASTAR*, *L*, and *ABAR* are constant, the fundamental frequency decreases with increasing *GSTAR*. This is expected since, with increasing *GSTAR*, the total bending stiffness (computed from *GSTAR*) decreases, and as a consequence, the fundamental frequency decreases.

4.3.2 Effects on "Optimal ABAR"

Figures 4.2 show the maximum dead load plus earthquake stresses (scaled by a reference stress of 22.0 ksi), in the arch and the deck, versus *ABAR*. The curves are rather flat. The optimal *ABAR* is the value of *ABAR* for which the stresses in the arch and those in the deck are equal. Table 4.2 summarize the optimal values of *ABAR*, taken from Figures 4.2, and the stresses corresponding to them. The optimal *ABAR* varies from 0.75 to 0.97, and is never larger than 1.0. When varying *L*, *ASTAR* and *GSTAR* respectively, the following points are noted:

1. "Optimal *ABAR*" is not sensitive to length, though generally, slightly decreasing with length. The corresponding stresses also generally decrease slightly with length.

2." Optimal *ABAR*" is not sensitive to *ASTAR*. However, the corresponding stresses obviously decrease with increasing ASTAR, i. e., increasing total area of deck plus rib.

3. "Optimal *ABAR*" generally decreases with increase in *GSTAR*; i. e., for a more flexible structure. The stresses also generally decrease slightly with increasing *GSTAR*.

As mentioned previously, the values of "optimal ABAR" presented in this study may be used as design aids in a preliminary decision on the

relative amounts of structural material to be used for the rib and the deck.

Table 4.1 Fundamental Frequency (ABAR = 1.0)

ASTAR = 1.00			
GSTAR	2.00	5.00	10.00
Span (ft)			
200.00	1.167	1.041	0.742
400.00	0.825	0.736	0.524
800.00	0.583	0.520	0.370
ASTAR = 2.00			
GSTAR	2.00	5.00	10.00
Span (ft)			
200.00	1.578	1.048	0.742
400.00	1.115	0.741	0.525
800.00	0.788	0.523	0.371
ASTAR = 3.00			
GSTAR	2.00	5.00	10.00
Span (ft)			
200.00	1.652	1.049	0.742
400.00	1.166	0.741	0.525
800.00	0.822	0.523	0.371

Table 4.2 Values of "Optimal ABAR" and Corresponding Stress

ASTAR = 1.0						
GSTAR	2.00		5.00		10.00	
Span (ft)	Optimal ABAR	$f_{DL}+f_{EQ}$ (ksi)	Optimal ABAR	$f_{DL}+f_{EQ}$ (ksi)	Optimal ABAR	$f_{DL}+f_{EQ}$ (ksi)
200.00	0.93	4.8	0.93	4.5	0.82	4.7
400.00	0.92	4.5	0.92	4.2	0.81	4.3
800.00	0.91	4.1	0.91	3.9	0.80	4.0
ASTAR = 2.00						
GSTAR	2.00		5.00		10.00	
Span (ft)	Optimal ABAR	$f_{DL}+f_{EQ}$ (ksi)	Optimal ABAR	$f_{DL}+f_{EQ}$ (ksi)	Optimal ABAR	$f_{DL}+f_{EQ}$ (ksi)
200.00	0.93	2.6	0.83	2.5	0.82	2.5
400.00	0.89	2.5	0.82	2.4	0.80	2.3
800.00	0.88	2.1	0.80	2.2	0.79	2.1
ASTAR = 3.00						
GSTAR	2.00		5.00		10.00	
Span (ft)	Optimal ABAR	$f_{DL}+f_{EQ}$ (ksi)	Optimal ABAR	$f_{DL}+f_{EQ}$ (ksi)	Optimal ABAR	$f_{DL}+f_{EQ}$ (ksi)
200.00	0.97	1.7	0.83	1.8	0.80	1.9
400.00	0.96	1.6	0.84	1.6	0.78	1.7
800.00	0.94	1.5	0.83	1.5	0.75	1.6

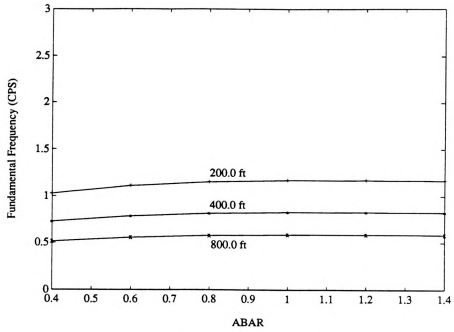

(a) ASTAR=1.0, GSTAR=2.0

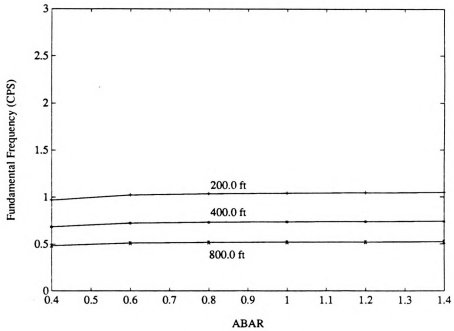

(b) ASTAR=1.0, GSTAR=5.0

Figure 4.1 Fundamental Frequency as a Function of ABAR

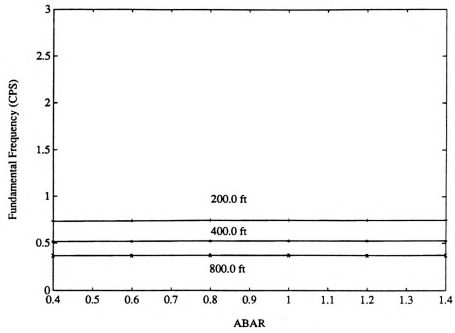

(c) ASTAR=1.0, GSTAR=10.0

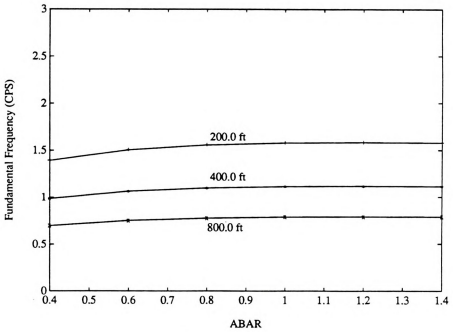

(d) ASTAR=2.0, GSTAR=2.0

Figure 4.1 Fundamental Frequency as a Function of ABAR (continued)

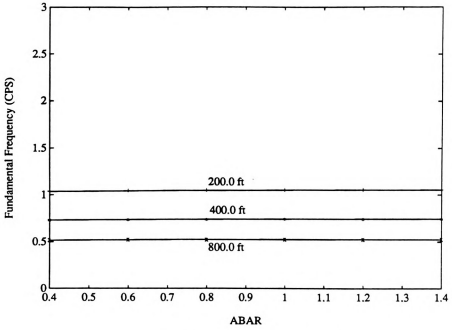

(e) ASTAR=5.0, GSTAR=5.0

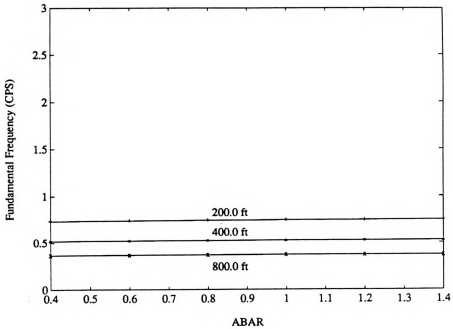

(f) ASTAR=10.0, GSTAR=10.0

Figure 4.1 Fundamental Frequency as a Function of ABAR (continued)

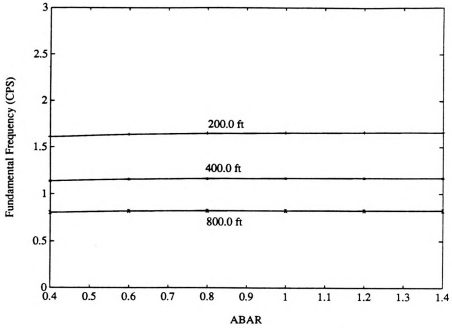

(g) ASTAR=3.0, GSTAR=2.0

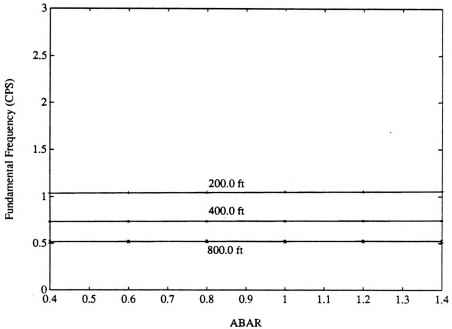

(h) ASTAR=3.0, GSTAR=5.0

Figure 4.1 Fundamental Frequency as a Function of ABAR (continued)

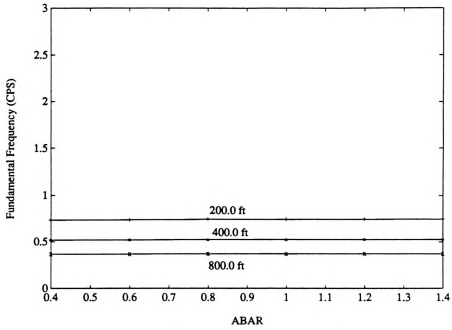

(i) ASTAR=3.0, GSTAR=10.0

Figure 4.1 Fundamental Frequency as a Function of ABAR (continued)

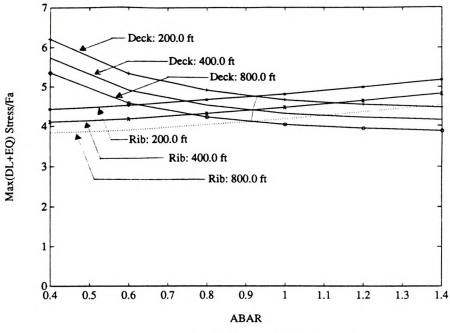

(a) ASTAR=1.0, GSTAR=2.0

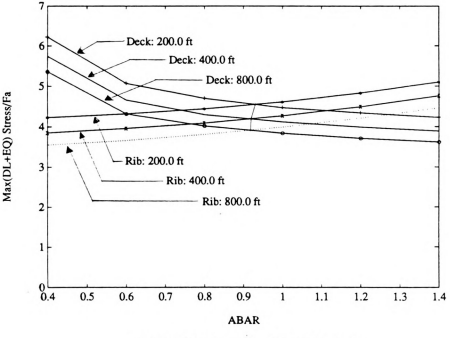

(b) ASTAR=1.0, GSTAR=5.0

Figure 4.2 Maximum Dead Load and Earthquake Stresses Versus ABAR

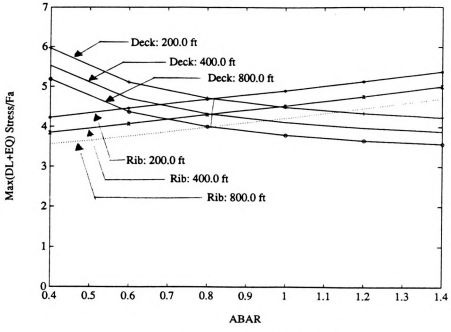

(c) ASTAR=1.0, GSTAR=10.0

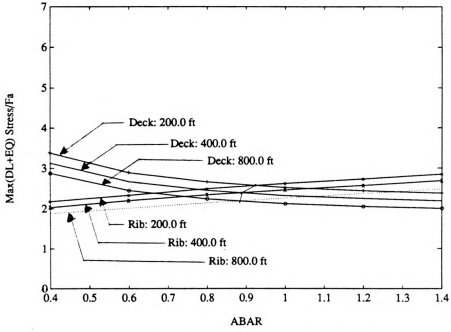

(d) ASTAR=2.0, GSTAR=2.0

Figure 4.4.2 Maximum Dead Load and Earthquake Stresses Versus ABAR

(continued)

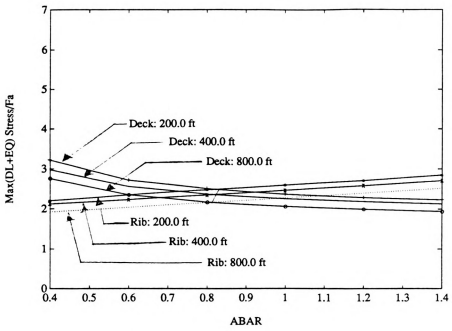

(e) ASTAR=5.0, GSTAR=5.0

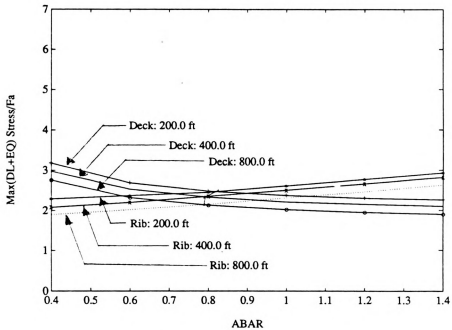

(f) ASTAR=10.0, GSTAR=10.0

Figure 4.2 Maximum Dead Load and Earthquake Stresses Versus ABAR

(continued)

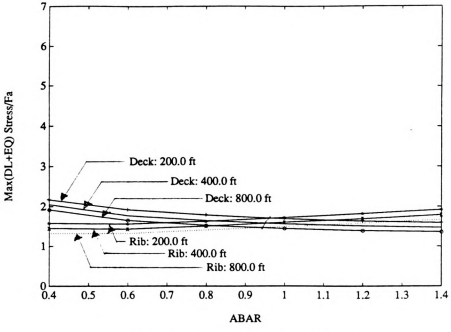

(g) ASTAR=3.0, GSTAR=2.0

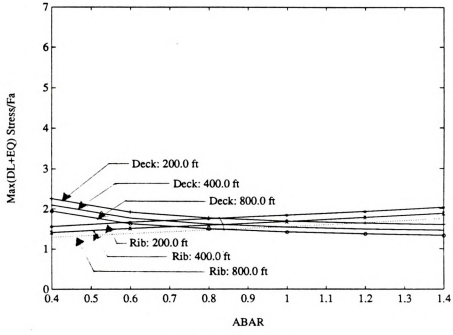

(h) ASTAR=3.0, GSTAR=5.0

Figure 4.2 Maximum Dead Load and Earthquake Stresses versus ABAR

(continued)

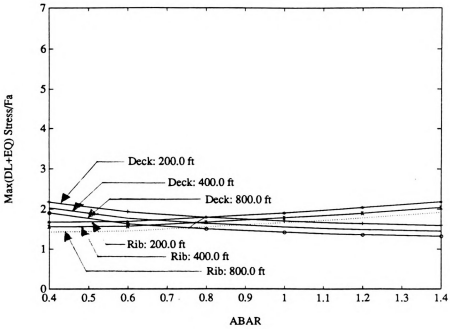

(i) ASTAR=3.0, GSTAR=10.0

Figure 4.2 Maximum Dead Load and Earthquake Stresses versus ABAR

(continued)

5. COMPARISON OF TIED AND DECK TYPE BRIDGES

5.1 General

In this Chapter, the response to seismic excitations of T-bridges is compared to that of D-bridges. The motivation to conduct this comparison is that most of the past work has been done on D-bridges. Relatively little research has been done on T-bridges. It would be of interest to compare the two types.

The D-bridge model is illustrated in Figure 5.1. The in-plane structure has a parabolic arch represented by a series of curved beam elements. The deck is represented by a series of straight beam elements. The columns connecting arch and deck are represented by truss elements. The bridge has eight panels of equal length. The arch is hinged at the supports, and the deck has roller supports. The cross-sectional area and the moment of inertia are assumed to be the same for each set of elements.

The D-bridge model (Figure 5.1) differs from the tied bridge model (Figure 2.1) in the following ways:

1. Most conspicuously, they differ in the location of the roadway relative to the arch. The deck of the D-bridge is above the arch, that of the T-bridge is beneath the arch. The arch and deck are connected at the arch crown in the D-bridge case. They are connected at the supports in the T-bridge case.
2. The D-bridge has a hinged rib, i.e., there is zero moment at either rib

supports. In the T-bridge case, in general, the rib has zero moment at the supports only if the deck beam has zero bending stiffness. That is due to the continuous connections between the rib and deck at the supports.

3. The deck of the D-bridge is on rollers. Under dead load, it has zero axial force.

The following is a comparison, first of the dead load response, then of the seismic response of the two bridge types, with the same set of reference parameters (set D): L=750.0 ft, H/L=0.175, M=4.80 kips/ft, M_r/M = 0.265, $GAMMA$=5.25, $(L/R)_c$ = 200.0, $ABAR$=0.688, C_r/R_r=1.275, C_d/R_d = 1.275. The varying parameter is RHO; the ratio of deck bending stiffness to rib bending stiffness. The range over which RHO is varied is: 0.0, 0.1, 0.2, 0.5, and 1.0, although, any values of RHO larger than 0.5, are probably of little practical interest in the case of D-bridges. At this point, it is important to mention which dimensional parameters change with RHO, and which remain fixed. For the data presented, the rib bending stiffness remains constant. With increasing RHO, the deck bending stiffness increases, and therefore, the total stiffness increases. Also, for the data presented the area of the rib increases. Since $ABAR$ is constant, the area of the deck also increases, and therefore, the total area increases. Summarizing, in the results presented in this chapter, with increasing RHO, I_d, A_d and A_r all increase, and I_r remains constant.

5.2 Fundamental Natural Frequency

Table 5.1 is a listing of the fundamental frequency of tied and deck type arched bridges for different values of RHO. For both bridge types the fundamental frequency increases with RHO. This is expected since the total structural stiffness increases with RHO. What seems unexpected is that the

fundamental frequency of the tied bridge is higher than that of the deck bridge. Initially, it is expected that the deck type bridge has higher fundamental frequency, because it corresponds to a tie-bridge with an infinite axial stiffness of the deck (tie). It seems superficially to be a stiffer structure, and thus should have a higher frequency. However, the results show that the deck bridge has a lower fundamental frequency than the tie bridge. The reason for this lies in the support conditions. For the horizontal degrees of freedom at the deck level, the D-bridge is more flexible than the T-bridge and hence has lower frequencies. In an attempt to prove this, the mass is removed from the deck. With mass on the rib only, the two bridges are similar for the horizontal degrees of freedom. Actually, the D-bridge is a little stiffer (both rib supports are hinged). As expected, the fundamental frequencies of the two bridges are very close. The frequency of the D-bridge is slightly higher (0.505 hetrz as opposed to 0.504 hertz for the T-bridge).

5.3 Dead Load Response

Figure 5.2 is a plot of the maximum dead load stresses among all point on the arch rib, similarly for the deck, for both tied and deck type bridges, versus *RHO*,i.e., the deck to rib bending stiffness ratio. The location of the various maximum stresses are noted in Tables 5.2 and 5.3 for the deck and the rib, respectively. For both bridge types, the maximum dead load stresses gradually decrease with increasing *RHO* values. This can be explained by the fact that both the total bending stiffness and the total area increase with increasing *RHO*, as mentioned earlier. Consequently, the stresses decrease. Thus, these trends seem obvious. But the relative responses for the various cases at given values of *RHO* are informative.

5.3.1 Stresses in the Deck

In the D-bridge case, the dead load stresses in the deck are small because the deck has roller supports, i.e., there is no axial load. All the stresses are due to bending. At zero value of *RHO*, there is no moment in the deck, the stresses are zero. For a positive value of *RHO*, there are some bending stresses, though small. As *RHO* increased from 0.0 to 0.1, the deck stresses increase for both types. Further increase in *RHO* results in a decrease in deck stress for the T-bridge. For the D-bridge, the stress remains essentially constant.

The deck dead load stresses in the T-bridge are much larger than those in the D-bridge. Those large stresses are mostly due to the axial tensile force in the T-bridge deck. The percentages of the T-bridge deck dead load stresses in bending are generally twice those of the D-bridge, as shown in Table 5.2. However, their actual magnitudes are much smaller than those due to axial force. Of course, the equivalent of that axial force is provided by the rib support horizontal reaction in the case of the D-bridge.

5.3.2 Stresses in the Rib

It is noted from Figure 5.2 that the stresses in the rib for the T-bridge and the D-bridge are quite close. This is because the rib behavior for the two bridges are typically of the arch kind. Although the sources of the horizontal thrust differ, the magnitude and effect are similar.

5.3.3 Sum of Deck and Rib Stresses

Also in Figure 5.2 is plotted the sum of the maximum dead load stresses among all points in the deck and among all points in the rib. For

both bridge types, as *RHO* increased from 0.0 to 0.1, rib stresses decreased by approximately the same amount as the deck stress increase, on the order of 5 percent. Since the rib stresses are similar for both bridges, the difference of the sum is similar to the difference in the deck stresses, discussed in section 5.3.1. The difference lies in the axial tensile force in the deck of the tie bridge.

5.4 Seismic Stresses

The maximum seismic stresses of both T-bridge and D-bridge are computed by use of the AASHTO spectrum. The maximum stresses and their location are listed in Tables 5.2 and 5.3. The results are plotted in Figure 5.3. The dead load stresses are not included in the seismic stresses discussed herein.

5.4.1 Stresses in the Deck

The seismic deck stresses in the D-bridge are not greatly different from those in the T-bridge, albeit smaller (Figure 5.3). As RHO increases from 0.0 to 0.1, the deck stresses increases for both bridge types. For RHO bigger than 0.1, the rate of increase drops rapidly. It is noted that for larger values of RHO, the values of the deck stresses for the two bridge types get closer.

5.4.2 Stresses in the Rib

As the deck stresses in the T-bridge are larger than the deck stresses in the D-bridge, the rib stresses in the T-bridge are smaller than the rib stresses in the D-bridge. For both bridge types, as RHO was increased from 0.0 to 0.1, the rib stresses decreased by approximately 10 percent. For RHO

bigger than 1.0, the rate of decrease drops. The stresses also get moderately closer with larger *RHO* values. It is interesting to look at the sum of the rib and deck stresses.

5.4.3 Sum of Deck and Rib Seismic Stresses

The sum of the seismic stresses in the deck and the rib for the two bridge types is close, with the D-bridge total stress moderately larger. It is noted that with increasing *RHO*, the deck stresses increase while the rib stresses decrease.

Table 5.1 Fundamental frequency of tied and deck type bridges

RHO	Fundamental Frequency (cps)	
	Tied Bridge	Deck Bridge
0.00	0.520	0.463
0.05	0.534	0.475
0.10	0.547	0.487
0.20	0.573	0.510
0.50	0.644	0.513
1.00	0.745	0.663

Table 5.2 Deck Maximum Stresses for Tied and Deck Type Arched Bridges

RHO	Bridge type	Maximum dead load stress (ksi)	M, I	SAM	Dead load bending stress (ksi)	Maximum seismic stress (ksi)	M, I
0.00	Deck bridge	0.0		0.00	0.00	1.30	4, 1
0.00	Tied bridge	3.89	1, 1	1.00	0.00	3.08	8, 1
0.05	Deck bridge	0.19	2, 1	0.00	0.19	2.39	3, 1
0.05	Tied bridge	4.21	1, 1	0.88	0.505	3.97	8, 1
0.10	Deck bridge	0.25	1, 2	0.00	0.25	2.98	3, 1
0.10	Tied bridge	4.19	1, 1	0.84	0.67	4.26	8, 1
0.20	Deck bridge	0.31	1, 2	0.00	0.31	3.62	3, 1
0.20	Tied bridge	4.02	1, 1	0.81	0.764	4.54	8, 1
0.50	Deck bridge	0.34	1, 2	0.00	0.34	4.15	3, 1
0.50	Tied bridge	3.41	1, 1	0.76	0.818	4.57	8, 1
1.00	Deck bridge	0.30	1, 2	0.00	0.30	4.00	3, 1
1.00	Tied bridge	2.65	1, 1	0.73	0.715	4.00	8, 1

Table 5.3 Rib Maximum Stresses for Tied and Deck Arched Bridges

RHO	Bridge type	Maximum dead load stress (ksi)	M, I	Maximum seismic stress (ksi)	M, I
0.0	Deck bridge	4.46	4, 2	8.29	2, 2
0.0	Tied bridge	4.73	5, 1	6.17	1, 2
0.05	Deck bridge	4.27	4, 2	7.82	2, 2
0.05	Tied bridge	4.50	4, 2	5.93	1, 2
0.1	Deck bridge	4.10	4, 2	7.39	2, 2
0.1	Tied bridge	4.33	5, 1	5.69	6, 1
0.2	Deck bridge	3.78	4, 2	6.64	2, 2
0.2	Tied bridge	3.99	5, 1	5.26	6, 1
0.5	Deck bridge	3.10	5, 1	5.04	2, 2
0.5	Tied bridge	3.24	4, 2	4.17	6, 1
1.0	Deck bridge	2.42	3, 2	3.53	2, 2
1.0	Tied bridge	2.50	5, 1	3.07	1, 2

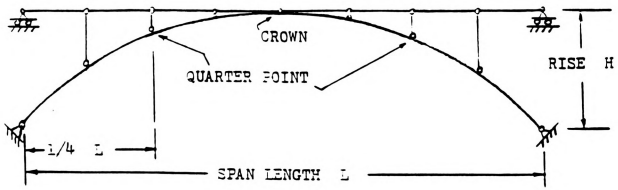

Figure 5.1 Deck Type Bridge Model

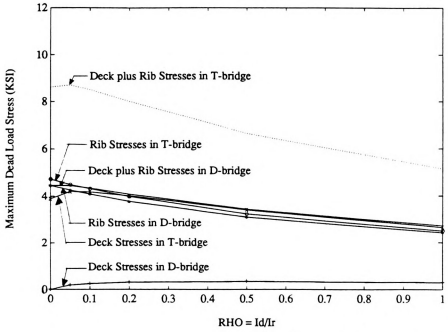

Figure 5.2 Maximum Dead Load Stresses of Tied Bridges and Deck Bridges

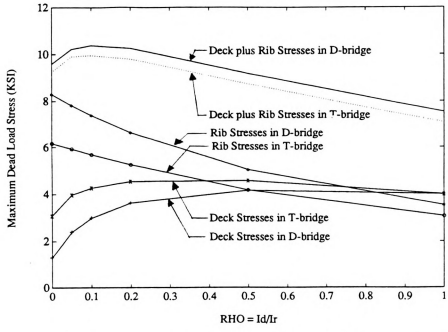

Figure 5.3 Maximum Seismic Stresses of Tied Bridges and Deck Bridges

6. CONCLUDING REMARKS

6.1. Recapitulation

There have been many works done on the seismic responses of the deck type arch bridges. On the tied type arch bridges however, it appears that only a single one [4] was reported, highlighting the modelling of the deck in its out-of-plane response. The work presented herein studies the seismic response of the tied type from a somewhat broader viewpoint, although it treats only in-plane response. It covers a number of real bridges and additional theoretical ones generated from parametric variations. A summary of the work done is presented in the following:

1. Seven existing tied arch bridges are classified, according to their design features into three types: heavy rib-light deck, light rib-heavy deck and medium rib-medium deck. From the parameters of these types, representative values of the parameters were defined for each type. Then a prototype was chosen for each type. It was used to generate two more bridges having the same volume of structural material, span length and dead load as the prototype, but otherwise with the representative parameter values of the other two types. Seismic responses of the three bridges were computed and compared. No major difference in the responses was found in terms of the dimensionless response quantities (stress amplification factors and displacement ratios).

2. Three ground motion inputs (the 1940 El Centro and the CIT B1 and B2 [6]) were used to compute the time history responses (stress amplification factor and displacement ratios). The time history analysis results were averaged and compared with spectral responses that were based on the AASHTO design spectrum. The responses obtained using the AASHTO response spectrum [5] were found to be very close to the average of the responses to the three time history ground motions. This suggests that the AASHTO design spectrum is a good representation of the earthquake loading for this type of bridge.

3. The earthquake effects were compared with live load effects by introducing a "structural zone factor" Z_{st}. This factor represents the live load effect in terms of earthquake effects. When Z_{st} is equal to unity, the live load effects are equivalent, from the design perspective, to the effects of earthquake with an intensity considered herein (AASHTO "bed-rock" acceleration equal to 0.4g and a "soil factor" equal to 1.0 [5]). If the value of Z_{st} for a given bridge corresponds to a greater seismicity than the site seismicity, then live load effects would be more critical than earthquake effects, and vice versa.

4. It was attempted to find an "optimal distribution" of structural material between the rib and deck. That distribution was assumed to be defined by an "optimal" value of ABAR, i.e., the ratio of cross-sectional area of deck to that of the rib, for which the maximum stress in the rib is equal to that in the deck. Based on this assumption and a further assumption that the bending stiffness ratio (of the deck to the rib) is equal to ABAR squared, an "optimal value" of ABAR was found for a range of parameters consisting of the length, the total cross-sectional area (of rib plus deck) and the total structural bending stiffness (of rib plus deck). The values of "optimal

ABAR" were found to be within the range of 0.75 and 0.97.

5. The responses of the T-bridges are compared with those of the D-bridges. The rib stresses of the T-bridge, for both dead load and earthquake load, are quite similar to those of the D-bridge. It appears that the structural behavior of the rib for the two types is almost the same, except that the horizontal thrust is provided by the tie in the T-Type bridge case, and by the rib support reaction in the case of the D-Type bridge. It appears that for the parameters considered (based on practical bridges), the axial elasticity of the deck apparently has a relatively small effect. A major difference in the deck stresses is that in the T-bridge, there is a substantial tensile stress to provide for the thrust needed by the rib.

The fundamental frequency for the D-Type bridge is lower than that of the T-Type bridge because of the smaller horizontal stiffness for the deck mass (deck on rollers at the ends in the case of the D-Type bridge, while the deck ends are rigidly connected to the rib in the case of the T-Type bridge). However, the difference is not major, being of the order of 10 percent.

6.2 Concluding Remarks

The most important limitation of the study is that it deals with two-dimensional structures only, i.e., in-plane response only. Nevertheless, as in the case of design for static loading, in-plane behavior in itself should be a major consideration in bridge design. To further limit the scope of the study, no structural-soil interaction is accounted for, and possible unequal support motions are also excluded from consideration. Most real bridges would have more than the eight panels that were used in this study. However, it is believed that eight panels would be sufficient to capture the

most important response characteristics. Larger number of panels would in all probability decrease the magnitude of the response approximately in the same manner as a larger number of more closely spaced loads replacing the statical equivalent of a lesser number of loads spaced farther apart. All in all, the difference should not be large, perhaps on the order of 10 percent.

The dead load plus earthquake stresses of the D-bridge deck seem somewhat greater than those of the T-Type bridge. The difference is however not major. This would suggest that one could use design aids for the D-bridges for the design of the T-bridges, at least as rough approximations.

The following is a list of suggestions for future study on the subject considered here.

1. In Chapter four, some "optimal design" aids were attempted for, based on the assumption that the stresses in the rib and deck are equal at an "optimal value" of *ABAR*. It would be interesting to conduct a study using a three dimensional model, and find some kind of optimization that includes the suspenders and the lateral beam and truss elements along with the rib and deck.

2. Also in Chapter four, the value of *RHO* was assumed to be equal to that of *ABAR* squared. It would be of interest to find and use different functions of *ABAR* for the value of *RHO*.

3. It would also be interesting to search for "optimal designs" for D-bridges and compare them with those for T-bridges.

LIST OF REFERENCES

1. Dusseau, R.A., and Wen, R.K., (1989), "Seismic Responses of Deck-type Arch Bridges," Earthquake Engineering and Structural Dynamics, Vol. 18, pp. 701-715.

2. Wen, R.K., and Lee, C.M., "Nonlinear Earthquake Responses of Arch Bridges," Ninth world Conference on Earthquake Engineering, 1988, Tokyo, Japan.

3. Millies, R.J., "Three-Dimensional Elastic Seismic Response of Deck-type Arch Bridges," M.S. Thesis, Department of Civil Engineering, Michigan State University, 1992.

4. Lee, H.E., and Torkamani, M.A.M., (1989), "Dynamic Response of Tied Arch Bridges to Earthquake Excitations," Department of Civil Engineering, University of Pittsburgh, Pittsburgh, Pennsylvania.

5. Standard Specifications for Highway Bridges 1983. American Association of State Highway and Transportation Officials. Section 3.15. Washington, D.C.

LIST OF REFERENCES (continued)

6. Jennings, P.C., Housner, G.W., and Tsai, N.C. (1968), "Simulated Earthquake Motions," Report to the National Science Foundation, California Institute of Technology.

7. Wen, R.K., and Suhendro, B. (1991), "Nonlinear Curved-Beam Element for Arch Structures." Journal of Structural Engineering, ASCE, 117(11), 3496-3515.

8. Merrit, F.S., Editor, "Structural Steel Designers' Handbook," section 13, McGraw-Hill Book Company, New York, 1972.

9. Lee, C.M., "Nonlinear Seismic Analysis of Steel Arch Bridges," Ph.D. Dissertation, Michigan State University, E. Lansing, MI, 1990.

10. Clough, R.W. and Penzien, J., "Dynamics of Structures," McGraw-Hill Book Company, New York, 1975.

11. Wen, R.K., Users' Manual for "NOALIST, a General Computer Program for Arch Bridges," in preparation, Department of Civil and Environmental Engineering, Michigan State University, East Lansing, MI.